CEOCOR DRESDEN – SECTOR A

Paper n. 09

A DSP-based Measurement Algorithm for Corrosion Monitoring and Diagnostics

Melania Allocca(1), Pasquale Arpaia(2), Mirna Urquidi-MacDonald(3)

(1) *Dipartimento di Ingegneria dei Materiali e della Produzione, Università di Napoli Federico II, P.le Tecchio, 80 - Napoli, 80125, Italy, Ph. ++39 3489367596 - ++39 0815317044, e-mail alloccaa@libero.it*

(2) *Dipartimento di Ingegneria, Università del Sannio, Palazzo Dell'Aquila Bosco Lucarelli, Piazza Roma, 82100 Benevento, Italy, Ph. ++39 0824 305817 Fax ++39 0824 305840, e-mail arpaia@unisannio.it, http://cds.unina.it/~arpaia/*

(3) *The Pennsylvania State University, Department of Engineering, Science and Mechanics, 203 C Earth and Engineering Science Building, University Park, PA 16801, USA, Ph: 814 863 4217, Fax: 814 863-7967,e-mail: mumesm@engr.psu.edu*

I. INTRODUCTION

At to date, monitoring electrolytic corrosion phenomena is still a stimulating challenge for safety. As an example, in gas pipeline networks of towns, also a small holiday in pipe can generate dangerous consequences to buildings and persons. In this case, for the corrosion monitoring system, the town underground is a remote and electromagnetically hostile environment, often affected by stray currents capable of centupling the corrosion rate. Thus, specific and effective automatic solutions are necessary, capable not only of measuring the corrosion speed, but also of diagnosing position and size of the metal loss, early.

Among experimental techniques of on-field corrosion monitoring, Electrochemical Impedance Spectroscopy (EIS) is still one of most reliable and affordable [1]-[7]. A small-amplitude sine wave is applied to the interface metal-electrolyte (electrode) in order to gather information about corrosion reaction kinetics. Alternative techniques, such as Electrochemical Noise (EN) [8]-[10], where spontaneous electrochemical potential and current are monitored, do not have a settled and unambiguous basic analytical structure. Thus, different interpretation of results, as well as unacceptable measurement uncertainty, arise, asking for further investigations [9]. Moreover, in the abovementioned field applications in hostile electromagnetic conditions, very-low amplitude signals (order of mV fraction) of electrochemical noise can not be extracted easily. Finally, if the problem of signal transportation to the measurement system on cables of several tens of meters length is considered, the scarce on-field application of EN, in spite of its fashion in research, can be explained.

However, also for EIS, a comprehensive interpretation of measurement result and diagnostics of corrosion phenomena is a task carried out mainly at laboratory level. Moreover, with diagnostics aims, impedance spectra can not be univocally related to different operating conditions (such as cathodic protection level, soil resistivity, and so on) or to damage characteristics (such as failure position, leakage area extension) in an easy way.

In this paper, a digital signal processing (DSP)-based monitoring and diagnostics algorithm [11], exploiting EIS and suitable for a low-cost on-field micro implementation [12]-[13], is presented, numerically characterized and experimentally tested.

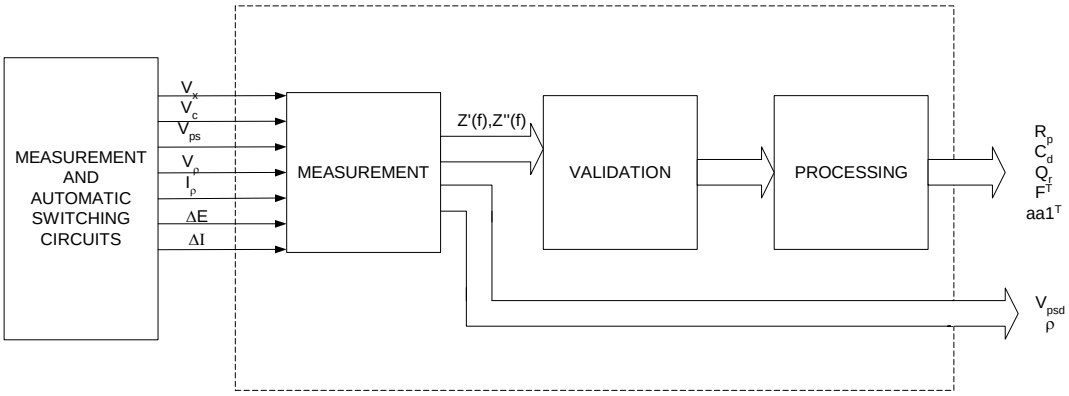

Fig.1 Architecture of the proposed micro corrosion meter.

II THE PROPOSAL

The proposed algorithm is implemented on a micro corrosion meter included in a distributed measurement system for corrosion monitoring and diagnostics [14]. The system is managed by an artificial neural network (ANN) [15]-[16], exploiting field data sent by the single micro corrosion meters distributed along the structure to be monitored.

A. Design concepts

The design of the proposed measurement algorithm for the micro corrosion meter was based on the main following concepts:

- Validation of electrical dynamic model of the corrosion phenomena directly on field, by means of Kramers-Kronig transforms [2]-[3], [6];
- In-deep analysis of diffusion and polarization corrosion phenomena, by means of piece-wise interpolation of impedance spectrum;
- Quantitative description of the impedance spectrum for the ANN work, by means of a shape analysis;
- Extraction of further hidden information inside the impedance spectrum, by means of wavelet transform [10], [17]-[18].

B. Architecture of the proposed micro corrosion meter

The architecture of the proposed micro corrosion meter implementing the above design concepts is shown in Fig. 1. It is based on three main blocks: measurement, validation, and processing. The first block measures (i) the voltage V_ρ and the current I_ρ, for the soil resistivity according to the Wenner method, (ii) the pipe-to-soil potential V_{PS}, (iii) the unknown V_X and reference V_C voltages, for measuring the real $Z'(f)$ and imaginary $Z''(f)$ parts of the impedance at the frequency f, according to a voltammeter digital method exploiting Hilbert transforms, proposed in [19], and (iv) the small variations of voltage ΔE and current density Δi, for assessing the anodic b_a and cathodic b_c Tafel constants [3]. Such quantities are obtained through suitable measurement circuits wired by an automatic switching unit.

From the measurement block, digital values of soil resistivity ρ, pipe-to-soil potential V_{PSD}, and real and imaginary parts of the impedance are obtained. Such data are filtered in the validation block by a suitable algorithm based on the Kramers-Kronig transforms [2]-[3], [6], and then

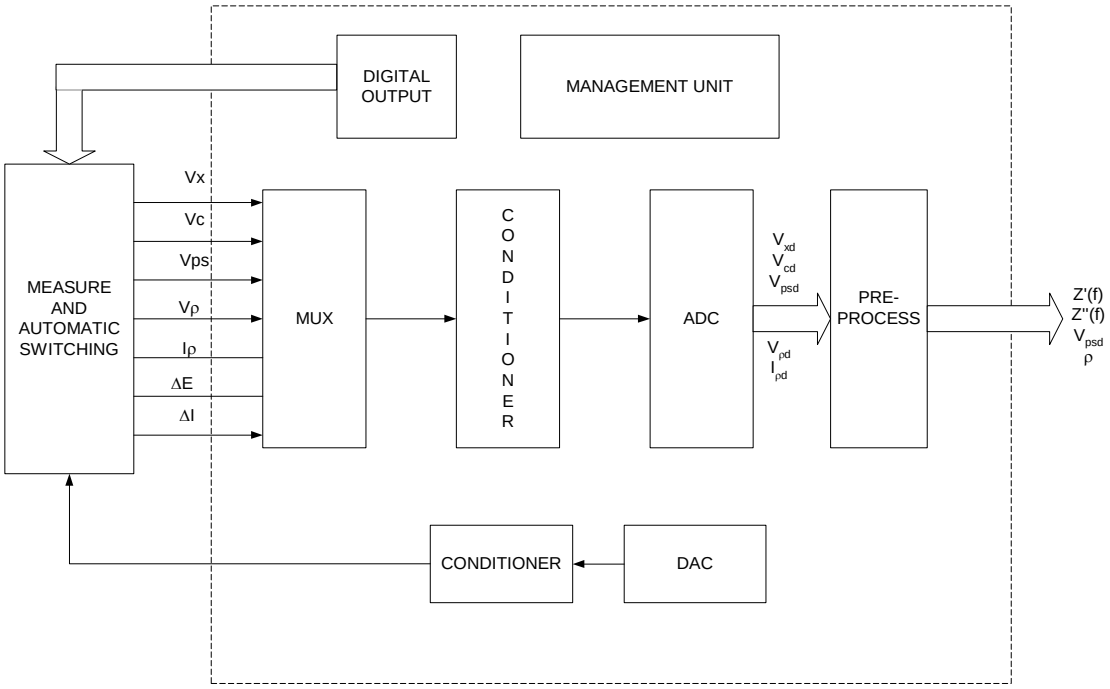

Fig.2 The measurement block

analyzed in the processing section in order to obtain the desired parameters for corrosion monitoring and diagnostics to be transmitted to the ANN.

Measurement block

The measurement block (Fig.2) consists of:

- a management unit to control the block as a whole;
- a digital port to drive the automatic wiring of the measurement circuits;
- a signal generator, consisting of a conditioning block and a DAC (digital-to-analog converter), generating a signal V_S, sinusoidal for impedance measurement, and dc for resistivity measurement;
- a multiplexer (MUX) selecting measurands according to the measurement to be carried out;
-a conditioner for the measurement signal;
- an ADC (analog-to-digital converter);
- a pre-processing unit, which computes the resistivity ρ, the pipe-to-soil potential V_{PSD}, and the real and imaginary parts of the impedance $Z'(f)$ e $Z''(f)$, (according to the Hilbert-based algorithm proposed in [19]) from the digital quantities $V_{\rho D}$, $I_{\rho D}$, V_{PSD} V_{XD}, V_{CD} (the digital measured values of V_ρ, I_ρ, V_{PS}, V_X, e V_C, respectively).

Validation block

A critical problem in EIS is data validation owing to uncertainty sources affecting experimental data, such as: not sufficiently low limit of the bandwidth, imperfect design of the electrochemical cell (faulty contact in electrodes, linking wires too long, and so on), or a too much selective FRA (filtering the nonsinusoidal response of the electrochemical system by linearizing its characteristic artfully).

Data were validated by verifying a significant coincidence with the ones modeled by Kramers-Kronig transforms (KK) [2]-[3], [6]:

$$Z_{KK}'(\omega) - Z'(\infty) = (\frac{2}{\pi})\int_0^{\infty} \frac{xZ''(\omega) - \omega Z''(\omega)}{x^2 - \omega^2} dx \quad (1)$$

$$Z_{KK}''(\omega) = -(\frac{2\omega}{\pi})\int_0^{\infty} \frac{Z'(\omega) - Z'(\omega)}{x^2 - \omega^2} dx \quad (2)$$

They stand if the electrochemical system fulfils the same main requirements (linearity, causality, stability) underlying the electrical impedance definition.

Processing block

Impedance data are interpolated in the frequency domain in order to increase the frequency resolution of the spectrum. In particular, interpolation requirements are different in the frequency bandwidth: (i) at low frequency (less than the Hz), possible diffusion phenomena (often of very low quantity) have to be detected and, simultaneously, high-variable amplitude noise due to measurement system has to be filtered; and (ii) at high frequency (more than the Hz), polarization phenomena have to be measured, and, thus, a more varying trend of the spectrum has to be approximated, with less influent noise. With this aim, a piece-wise interpolation according to frequency sub ranges was carried out (Piece-Wise Interpolation block, PWI in Fig.3). Further details on this procedure will given in the final paper.

Then, the interpolated data $Z'(f)_{INTERP}$ and $Z''(f)_{INTERP,}$ and the other measurement results are processed in order to compute:

- The polarization resistance R_p [3]:

$$R_p = \left(\frac{2}{\pi}\right)\int_0^{\infty}\left[\frac{Z''(x)}{x}\right]dx \approx \left(\frac{2}{\pi}\right)\int_{x\min}^{x\max}\left[\frac{Z''(x)}{x}\right]dx \quad (3)$$

- The corrosion current density i_c [3]:

$$i_c = \frac{B}{R_p} = \frac{(\Delta E)}{R_p(\Delta i)_{\Delta E \to 0}} \quad (4)$$

where B is a constant taking into account the anodic b_a and cathodic b_c Tafel constants*:*

$$B = \frac{b_a * b_c}{2.3*(b_a + b_c)} \quad (5)$$

- The corrosion speed v_c [3]:

$v_c = i_c$ K EW/dA (6)

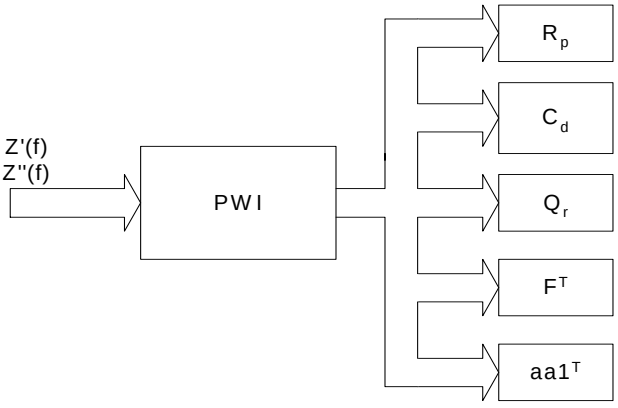

Fig.3 Processing block

where i_c is the corrosion current density in Ampere/cm^2, K is a unit conversion constant, EW is the equivalent weight in equivalent grams, d is the density in grams/cm^3, and A is the holiday area in cm^2;

- The double-layer capacity C_d [3]:
  $C_d = 1/[2\pi f R_p]$ (7)
- The coating quality index:
  $Q_R = \max(Z''(f)_{INTERP})/ R_p$ (8)
  giving an idea of the coating quality in the area invested by the measurement signal; when Q_R is equal to 1, there are no holidays, when is less than 1, a loss in the coating is present.

The shape of the spectra $Z'(f)_{INTERP}$ and $Z''(f)_{INTERP}$ can discriminate some corrosion conditions better than the Bode and Nyquist representations. In particular, the following points (the array F^T in Fig.3) were determined in order to describe these spectra quantitatively:

- F_1, F_2 and F_3, on the imaginary part spectrum $Z''(f)_{INTERP}$, aimed at measuring corrosion phenomena of polarization and diffusion. The points F_1 and F_3 correspond to two maxima and F_2 to the inflection point between them (Fig.4b). In case of a significant diffusive behavior, a bimodal spectrum is obtained, with a first local maximum (F_1) at low frequency (corresponding to the maximum of a first Nyquist circle), and a second local maximum (F_3), pointing out higher frequency polarization phenomena (corresponding to a second Nyquist circle). Without a diffusive behavior, only one global maximum arises (F_1), and, in this case, the algorithm selects the last spectrum point as F_3;
- F_4, F_5, and F_6, on the real part spectrum $Z'(f)_{INTERP}$, for detecting polarization phenomena specifically; F_4 and F_6 correspond to the two sharp ends at higher frequency and F_5 to the inflection point between them (Fig.4c).

The real part spectrum $Z'(f)_{INTERP}$ turns out to be less variable with the measurement conditions than the imaginary part one (Fig 4c). Thus, more detailed information was extracted through a wavelet transform [17]-[18]. The peculiar stepwise shape of $Z'(f)_{INTERP}$ suggested the use of a mother haar. The DWT decomposition was stopped at the first level in order to (i) determine the general half-band haar-like trend of the spectrum (analysis of bigger shape variations, i.e. on larger frequency scale) through the approximation coefficient spectrum, and (ii) to extract particular half-band haar-like information (analysis of smaller shape variations, i.e. on smaller frequency scale), sometimes not perceptible on the spectrum, through the detail coefficient spectrum.

III PRELIMINARY EXPERIMENTAL RESULTS

A measurement station on a pilot plant was set-up at Penn State University [20], in order to carry out experimental tests in reference conditions of: (i) soil resistivity, (ii) coating holidays, (iii) cathodic protection, and (iv) electrode positions.

In particular, a test campaign was carried out in order to validate the proposed measurement algorithm, according to the following plan, repeated twice for high () and low (20 kΩ cm) resistivity soils:

- In absence of holidays:
  - Assessment of the cathodic protection influence;
  - Assessment of the electrode position;

- In presence of holidays:
    - Assessment of the cathodic protection influence;
    - Assessment of the electrode position.

In the full paper, three main examples of test results are reported, aimed at showing the proposed algorithm performance, by referring to the main design concepts of (i) piece-wise frequency interpolation, (ii) shape analysis, and (iii) use of the wavelet transform.
In the following, for the sake of the brevity, the discussion of only one of the three cases is reported (Fig.4).
The low-frequency small tails on the right side of the Nyquist plots in Fig. 4a (*NP* and *CP*: without and with cathodic protection, respectively) show a diffusive behavior of the electrochemical system. The design idea of different interpolations in the frequency range of the real and imaginary part spectra allows (i) a first local maximum at low frequency, pointing out a diffusion phenomenon, and (ii) a second maximum at high frequency, pointing out a polarization phenomenon, to be detected easily on the imaginary part spectrum (Fig. 4b). These two points are also the shape factors *F1* and *F3*, while *F2* is the inflection point between them. The set of the 3 points (Table 4f) describes the trend of the imaginary part spectrum synthetically in a quantitative way for successive processing by the ANN. Analogously, the points *F4*, *F5*, and *F6* (Fig. 4c and Table 4f) describe the polarization behavior, evident in the real part spectrum at visual level, in a quantitative and synthetic way. However, the same spectrum does not point out the diffusive behavior at low level, and a wavelet transform is carried out (Figs. 4d and 4e). In particular, the detail coefficient spectrum (Fig. 4e) shows the diffusion at low frequency clearly. Moreover, it allows the difference between the 2 real part spectra (*NP* and *CP*) in the inflection point *F5* to be detected, in spite of its amount, less bigger than the uncertainty band. Apart other quantities C_d and Q_R estimated by the algorithm, Table 4g shows how the percentage error in the estimate of the polarization resistance R_p is about null.

ACKNOWLEDGEMENTS

This paper is dedicated to the late prof. Mario Arpaia, in the tenth anniversary of his death.
Authors thank dr. Homero Castaneda Lopez for gathering experimental results [20].
The work was supported on behalf of Università di Napoli Federico II, “Short Mobility Research Program”, July. 2002. Any commercial exploitation of the results of the present research is restricted to preliminary formal agreement with the Technology License Office of Penn State University.

REFERENCES

[1] M. Arpaia, G. Trisciuoglio, ”Identification of the electrical equivalent circuit for steel/concrete interface”, IMEKO TC-4 Symp. on Measurement and Estimation, Brixen, 1984.
[2] M. Urquidi-Macdonald, S. Real, D. D. Macdonald, "Application of Kramers-Kronig Transforms in the Analysis of Electrochemical Impedance Data. II Transformations in the Complex Plane," *J. Electrochem. Soc*., vol. 133, pp. 2018, 1986.
[3] J. R. Macdonald, Impedance Spectroscopy, John Wiley & Sons, New York, 1987.
[4] F. Mansfield, “EIS as a new tool for investigating methods of corrosion protection”, *Electrochimica Acta*, Vol. 35, No 10, pp 1533-1544, 1990.
[5] D. D. Macdonald, M. C. H. McKubre, and M. Urquidi-Macdonald, "Theoretical Assessment of AC Impedance Spectroscopy for Detecting Corrosion of Rebar in Reinforced Concrete," *Corrosion*, Vol. 44, No 2, 1988.

[6] M. Urquidi-Macdonald, S. Real and D.D. Macdonald, "Application of Kramers-Kronig Transforms in the Analysis of Electrochemical Impedance Data. II Stability, Causality, and Linearity", *Electrochimica Acta*, vol. 35, p. 1559 1990.

[7] A. Carullo, F. Ferraris, M. Parvis, A. Vallan, E. Angelini, P. Spinelli, "Low-cost Electochemical Impedance Spectroscopy System for Corrosion Monitoring of Metallic Antiquities an Works of Art", *IEEE Trans. on Instrum. and Meas.* ,Vol. 49, No 2, April, pp. 371-375, 2000.

[8] K.Hladky, J.L.Dawson "The Measurement of Localised Corrosion Using Electrochemical Noise", *Corrosion Science*, Vol. 21, No 4, pp. 317-322, 1981.

[9] A. Lowe, H. Eren, Y. J. Tan, B. Kinsella, S. Bailey, "Continuous Corrosion Rate Measurement by Noise Resistance Calculation", *IEEE Trans. on Instrum. and Meas.*, Vol. 50, No 5, Oct., pp. 1059-1065, 2001.

[10] A. Lowe, H. Eren, "Corrosion Signal Processing Using Wavelet Analysis and Nyquist Diagrams", IEEE IMTC-2002, Anchorage, 21-23 May, 2002, pp.855-860.

[11] M. Allocca, Diagnostics and monitoring of electrolytic corrosion phenomena in metallic materials: a DSP-based measurement algorithm, (in Italian) MD Thesis in Material Engineering, (D. Acierno, P. Arpaia, M. Urquidi MacDonald advisors), University of Napoli Federico II, 12th December 2002.

[12] A. Baccigalupi, C. Landi, "Single Chip Microcontrollers for Measurements on Rotating Electrical Machines", Int. Conf. on Electrical Machines ICEM, pp. 7-10, 1988.

[13] P.Arpaia, C. Landi, "A Microcontroller-based System for Pipe-to-Soil Potential Measurement", *Measurement and Control*, Vol.23, No 8, October, pp.237-241, 1990.

[14] P.Arpaia, F.Cennamo, P.Daponte, M.Savastano, "A Distributed Laboratory Based on Object-Oriented Measurement Systems", *Measurement*, vol.19, n.3-4, November-December, 1996, pp.207-215.

[15] A.C. Ramamurthy, M. Urquidi-Macdonald, "Application of Artificial Neural Network as Predictive Tools for Corrosion in Painted Automotive Substrates," SAE International, Dearborn, Michigan, paper 932337, October 4-6, pp 101-115, 1993.

[16] M. Urquidi-Macdonald and D.D. Macdonald, "Performance Comparison between a statistical model, a deterministic model, and an Artificial Neural Network model for prediction damage for pitting corrosion," NIST, Vol. 2, 1994.

[17] G. Strang, T. Nguyen, Wavelets and filter banks, Wellesley-Cambridge Press, 1996.

[18] L.Angrisani, P.Daponte, M.D'Apuzzo, A.Testa, "A measurement method based on the wavelet transform for power quality analysis," *IEEE Trans. on Power Delivery*, vol.13, No.4, Oct., pp.990-998, 1998.

[19] P. Arpaia, R. Schiano Lo Moriello, "A Digital Method based on Minimax FIR Filtering for Impedance Measurement, ISCS-01, Napoli, December, 2001.

[20] H. Castaneda Lopez, Location of coating defects and assessment of level of cathodic protection on underground pipelines using ac impedances, deterministic add nondeterministic models, PhD Thesis in Material Engineering, (M. Urquidi MacDonald advisor), Penn State University, 2001.

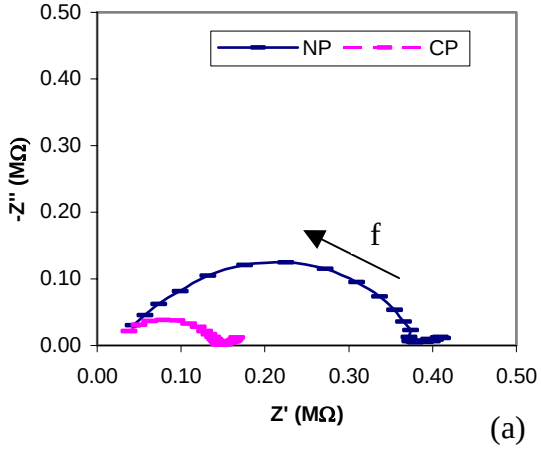

(a)

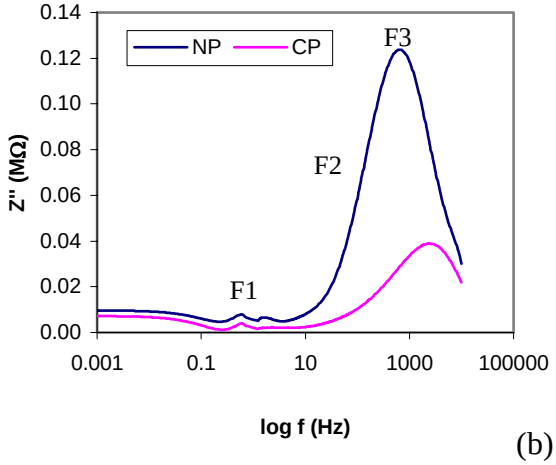

(b)

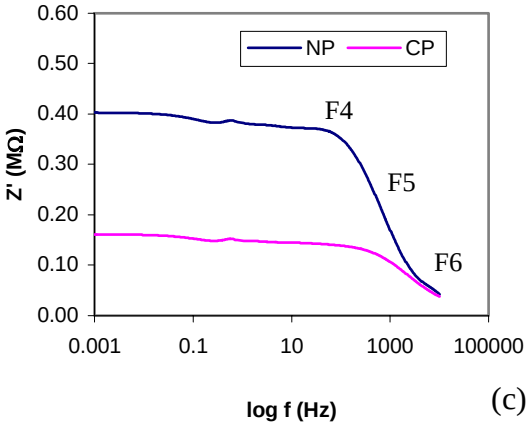

(c)

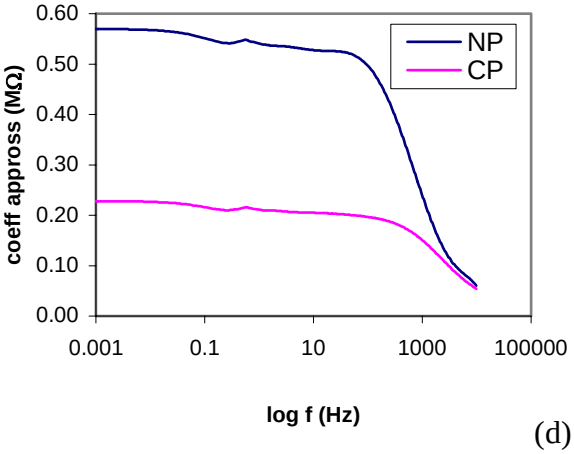

(d)

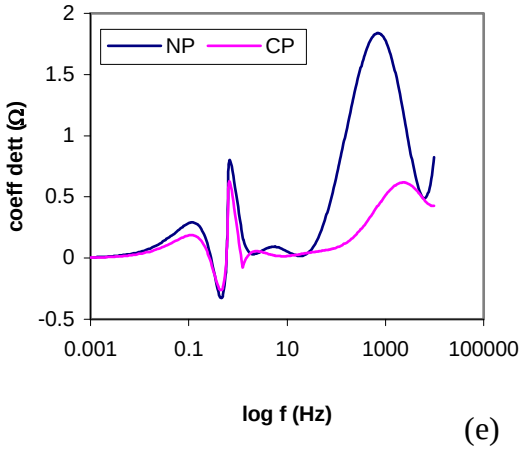

(e)

	NP		CP	
	(Hz)	(MΩ)	(Hz)	(MΩ)
F1	0.225	0.004	0.246	1214
F2	148.9	0.077	555.4	0.027
F3	648.4	0.12	2418	0.039
F4	63.55	0.36	152.8	0.14
F5	700.6	0.20	2296	0.080
F6	10000	0.042	10000	0.038

(f)

	R_{PRIF} (MΩ)	RP (MΩ)	ERRORE%	Cd (nF)	Q_R
NP	0.33	0.33	0.01	0.76	0.38
CP	0.11	0.11	0.00	0.64	0.37

(g)

Fig.4 (a) Nyquist diagram, (b) imaginary part spectrum, (c) real part spectrum, (d) wavelet transform by mother haar of the real part: approximation coefficients, (e) wavelet transform by mother haar of the real part: detail coefficients, (f) shape factors, (g) polarization resistance values: reference R_{pRIF} and measured R_p, double layer capacity C_d and coating quality index Q_R , in the frequency range (10^{-3}-10^4 Hz), 1 holiday, electrode in position 4X, low-resistivity soil (20 kΩ cm) as a function of the cathodic protection (NP: not protected, CP: protected).